MODELING OF MULTITURN INJECTION AT SIS-18 FOR A TRAIN OF UNILAC MICROBUNCHES

A. Lauterbach[1], G. Franchetti[2,3]
[1]Goethe University, Frankfurt, Germany
[2]GSI Helmholtzzentrum für Schwerionenforschung GmbH, Darmstadt, Germany
[3] Helmholtz Research Academy Hesse for FAIR (HFHF), Frankfurt, Germany

Abstract

Multiturn Injection is an essential tool for achieving high beam intensities in synchrotrons. At SIS-18, a significant increase in the intensity of the uranium beam is foreseen, by several orders of magnitude, up to 1.5×10^{15} ions per injection cycle, prior to acceleration and extraction to SIS-100. Under these conditions, any beam losses during injection become critical, both in terms of beam lifetime and the risk of damaging injection system components, in particular the electrostatic septum. Usually, the optimization of the multiturn injection is carried out considering only the process of injecting one transverse slice of UNILAC macroparticles per turn. We present here a three-dimensional modeling of the injection process, which takes into account the longitudinal structure of the injected beam, namely the train of microbunches, and evaluates differences from previous approaches.

ONE- AND TWO-PLANE MULTITURN INJECTION

In this study, we focus on the well implemented process of multiturn injection in one transverse plane, which has been subject of extensive research in the past [1–3], as well as the process of two-plane multiturn injection, which optimizes the painting of the phase space in both transverse planes and is subject of recent studies [4, 5]. In both cases, the transverse trajectory of the closed orbit center is excited via four steerer magnets, performing a local orbit bump, which enables collecting the beamlets injected outside of the electrostatic septum (ES). This accumulation process is also referred to as phase space painting.

Local Orbit Bump Decrease Functions

The bump amplitude is shaped by an initial maximum $u_{B,\mathrm{max}}$ and a decrease rate per turn, given by a decrease function f. For this work a linear decrease function f_1 is chosen for the one-plane MTI, based on the real bump decrease curve of the SIS18, and an exponential decrease function f_2 for the two-plane MTI, based on the current benchmark of two-plane multiturn injection studies at GSI [4], with $f_1 = u_B(i_t) = u_{B,\mathrm{max}}(1 - \frac{i_t - 1}{j})$, with u being the generalized transverse coordinate standing for x or y correspondingly, i_t the turn number and j being the number of turns until the orbit has decreased back to zero amplitude. For the purpose of this work we set j to the number of injection turns i_{inj}. For the two-plane MTI the decrease function is $f_2 = u_B(i_t) = b_u + (u_{B,\mathrm{max}} - b_u)\frac{1-e^{\tau_u(N_u - i_t)}}{1-e^{\tau_u N_u}}$ with b_u the plateau value the function approaches after N_u turns and τ_u is the exponential decay coefficient defining the shape and steepness of the curve.

Simulation Prerequisites

The injection coordinates of the bunches are set by $X'(s_{\mathrm{inj}}) = X(s_{\mathrm{inj}})[-\alpha_x(s_{\mathrm{inj}})/\beta_x(s_{\mathrm{inj}})]$, where $\alpha(s_{\mathrm{inj}})$ and $\beta(s_{\mathrm{inj}})$ are the Twiss parameters at the longitudinal injection location s_{inj}. For the purpose of this work we implemented a one-plane MTI simulation code in Fortran 2018, utilizing the MICROMAP library for beam initialization and tracking. The SIS18 lattice was used as a representative synchrotron lattice. The code initializes a beamlet at the longitudinal injection point at each turn and performs the corresponding local orbit bump. The particle coordinates are tracked throughout the injection process. Losses are checked at every calculation step, also for $i_t > i_{\mathrm{inj}}$ to check for after-injection losses with $i_{t,1\mathrm{P}} = 100$ and $i_{t,2\mathrm{P}} = 30$. The fixed simulation settings are shown in Table 1. Simulations are performed for two different tune sets “Q1” (Qx = 4.238, Qy = 3.422) and “Q2” (Qx = 4.290, Qy = 3.290). The selected tune sets enable an exploratory study while keeping the computational effort reasonable. A systematic tune scan is left for future work. Although septum thickness and field errors would be expected to increase the absolute particle losses, they are not expected to alter the qualitative comparison presented here and are therefore neglected. Space charge effects are not included in this work. Consequently, we neglect the induced tune spread, which would affect the present optimization of the bump ramp for the machine tunes used in this work. The reevaluation of this scenario including space charge is part of further work.

MODELING OF MICROBUNCH TRAIN

In regular MTI simulations, the injected particle bunches are often modeled as a single beam slice per turn, where a number N_p of particles is distributed transversely over the phase space area of the slice, in the exact same longitudinal position s. In this work, we want to model the longitudinal extension of the beamlets as a train of beam slices, in the following also referred to as “bunches” that are injected with a certain time delay Δt after one another. The ratio $\Delta t/t_{rev}$ corresponds to $i_s/i_{s,max}$, with i_s being the number of calculation steps between injections and $i_{s,max}$ the maximum

Table 1: Shared simulation settings for multiturn injection in this work for SIS18-lattice with U^{238}_{28+} ions. *) The $\Delta p/p$ value is scaled by a Gaussian random value in range [-1, 1].

Parameter	**Value**	**Unit**	**Description**
N_p	100	[1]	Particles per beamlet
i_{inj}	22	[1]	injected beamlets
ϵ_x (injection)	6	[mm-mrad]	Emittance, x-plane
ϵ_y (injection)	6	[mm-mrad]	Emittance, y-plane
Distribution	Gauss(3σ)	[-]	Beam-Distribution
$\Delta p/p*$	2.5×10^{-3}	[-]	Momentum Spread
E_{nuc}	11.4	[MeV/u]	Energy per nucleon
$\alpha_x(s_{Septum})$	-1.3862	[rad]	Twiss α, x-plane
$\beta_x(s_{Septum})$	14.919	[m]	Twiss β, x-plane
For 2-Plane MTI:			
θ	45	[deg]	Septum tilt angle
$\alpha_y(s_{Septum})$	-0.66484	[rad]	Twiss α, y-plane
$\beta_y(s_{Septum})$	10.517	[m]	Twiss β, y-plane

number of calculation steps within one turn and t_{rev} the revolution time of a particle at injection energy.

Injection Efficiency

For the purpose of this work, the injection efficiency is defined as $\eta = \frac{N_{p,\text{end}}}{N_{p,\text{inj}}}$, with $N_{p,\text{end}}$ being the number of particles that are not lost during injection, and $N_{p,\text{inj}}$ being the number of all particles that were initialized within the simulation. A particle is lost once one of its coordinates exceeds acceptance boundaries, especially near the septum.

Equidistant vs. Fixed-Distance Bunch Injection

The model shown in this work contains two schemes of injecting a number i_b of bunches longitudinally across the accelerator's circumference within one revolution: Equidistant injection (EQ) of i_b bunches per turn, and injection of i_b bunches per turn with a fixed distance (FX) of i_s calculation steps. Figure 1 shows a schematic view of both models.

In the EQ model i_s is calculated by $i_s = \text{int}(i_{s,max}/i_b)$. In the FX model i_s is a direct input for the code. Bunches are initialized every i_sth step as long as the number of bunches within one turn does not exceed i_b. The bunch frequency at the end of the transfer channel of the UNILAC is $f = 36.136$ MHz [6]. With $T = 1/f \approx 27.8$ ns. The distance Δs is equal to vT, with v being the velocity $v = \beta c$. Taking into account a relativistic β of 0.156, which corresponds to the injection energy of 11.4 MeV we get $\Delta s \approx 1.3$ m. The length l_s of SIS-18 is 216.72 m, thus Δs is $\approx 1/167$ of the complete accelerator circumference. Unlike in conventional studies, in this work the local orbit bump will be updated at every calculation step, providing a slightly different value to each of the bunches. A larger number of calculation steps creates a smoother bump curve. As a trade-off between precision and computational effort, we chose $i_{s,max} = 336$ per turn, keeping it an integer multiple of $l_s/\Delta s$. Injection is performed at every second step as an equivalent of an injection every $\Delta t = \Delta s/v_p$ with v_p being the particle velocity. This leads to a minimum distance between bunch centers of ≈ 1.29 m. Whilst the bunches are injected, the bumper flank is decreasing, leaving all bunches with a slightly different oscillation amplitude around the corresponding center of the closed orbit.

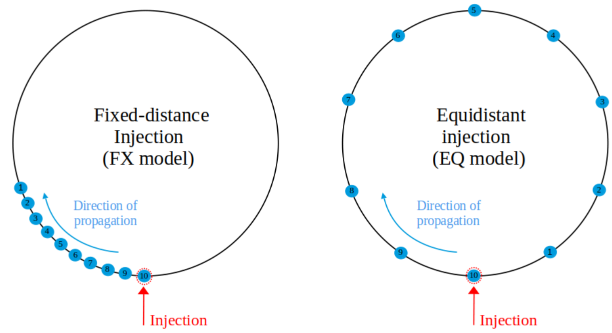

Figure 1: Schematic comparison of fixed-distance injection and equidistant injection for an example number of 10 beam bunches.

RESULTS AND DISCUSSION

This work evaluates a total of 16 simulation runs with different parameter settings. Table 2 summarizes the results, showing the efficiency for single-bunch injection ($i_b = 1$), the maximum achieved efficiency η_{max} with the corresponding number of injected bunches, as well as the gain in efficiency relative to the single-bunch case. The results are visualized in Fig. 2 for the one-plane MTI and in Fig. 3 for the two-plane MTI. Each plot shows the injection efficiency η as a function of the number of injected bunches i_b for the two bunch distribution schemes (FX and EQ), with and without momentum spread ($\Delta p/p$), as defined in Table 1.

Table 2: Simulation results with the highest efficiencies η simulated, displaying the maximum efficiency η_{max} for all simulation models (1P/2P:1-plane/2-plane, FX/EQ: fixed-distance/equidistant injection, tunes(Qx/Qy): Q1(4.238/3.422), Q2(3.290/4.290), and the corresponding bunch numbers with (d1) and without (d0) $\Delta p/p$ and the maximum gain in efficiency in percentage points).

Model	$\eta_{(i_b=1)}$[%] (d0 | d1)	η_{max}[%] (d0 | d1)	i_b[1] (d0 | d1)	$\Delta\eta_{max}$ [pt.] (d0 | d1)
1PEQQ1	59.59 | 57.73	60.67 | 58.71	5 | 3	1.08 | 0.98
1PFXQ1	59.59 | 57.73	60.08 | 58.55	167 | 2	1.41 | 2.08
1PEQQ2	65.32 | 59.68	66.73 | 61.76	18 | 57	0.99 | 0.82
1PFXQ2	65.32 | 59.68	66.33 | 61.45	168 | 168	1.01 | 1.76
2PEQQ1	82.23 | 79.32	82.75 | 80.94	85 | 3	0.52 | 1.62
2PFXQ1	82.23 | 79.32	82.72 | 80.63	90 | 4	0.64 | 1.71
2PEQQ2	74.68 | 73.14	75.32 | 74.85	85 | 3	0.54 | 1.31
2PFXQ2	74.27 | 72.86	75.19 | 74.38	90 | 4	0.92 | 1.51

The results show generally lower efficiencies when momentum spread is included, due to chromaticity and dispersion effects, which increase the effective emittance of the bunches and lead to enhanced particle losses at the ES.

The FX and EQ models coincide for one-plane MTI for $i_b = 1$ and $i_b = i_{b,\max} = 168$, as the bunch injection positions are similar for both models, see Fig. 2.

For intermediate values $1 < i_b < i_{b,\max}$, the FX model results in lower efficiencies than the EQ model for both sets of tunes. Tune set Q2 yields higher efficiencies for the one-plane MTI than Q1 (see Fig. 2). The Two-Plane MTI (2P) has its maximum value for $i_b > 1$, but remains below the maximum efficiency for Q2, which has higher difference in fractional tunes q_x and q_y, leading to a different sequence of phase advances μ_x and μ_y. The underlying behavior of the two-plane-injection is governed by the phase advance sequence $\mu_{x/y}(i) = i \cdot 2\pi q_{x/y}/i_b$, which defines the relative betatron phase of two successively injected bunches and therefore influences the way the phase space is populated in both transverse planes during the injection process, with i being the number of injections and q the fractional tune.

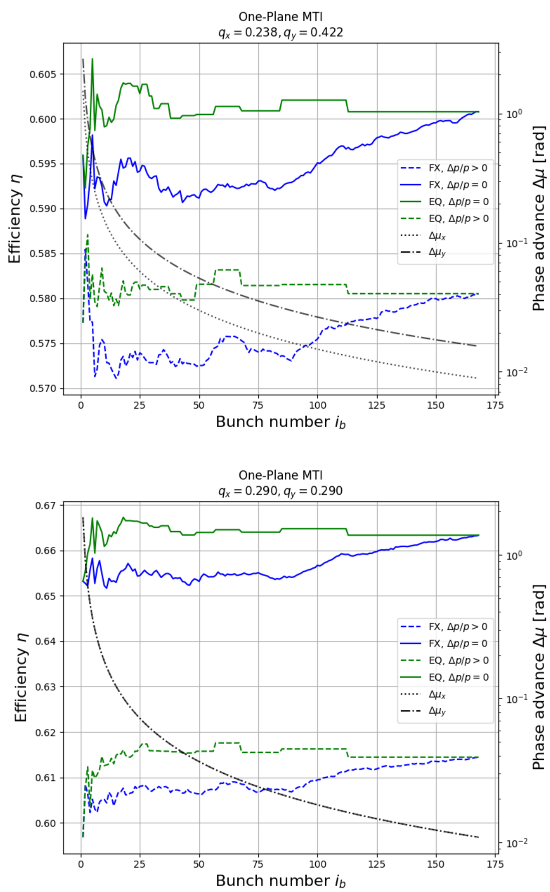

Figure 2: Comparison of FX- and EQ-bunch models with one-plane-MTI for two different tune sets: Injection efficiency η vs. number of bunches i_b with and without momentum spread $\Delta p/p$. The black curves indicate the phase advance between successive injections for the corresponding tune set.

For all combinations of models and tune sets, the EQ model results in slightly higher efficiency. The plateau in efficiency curves for the EQ model exhibited at larger values of i_b is caused by the discretization due to the finite step size of the simulation, which can be mitigated by increasing the computational effort. Even though efficiency gain with the new models is modest, an increase of one percentage point can already provide a valuable increase of transmitted intensity in high-intensity operations of SIS-18.

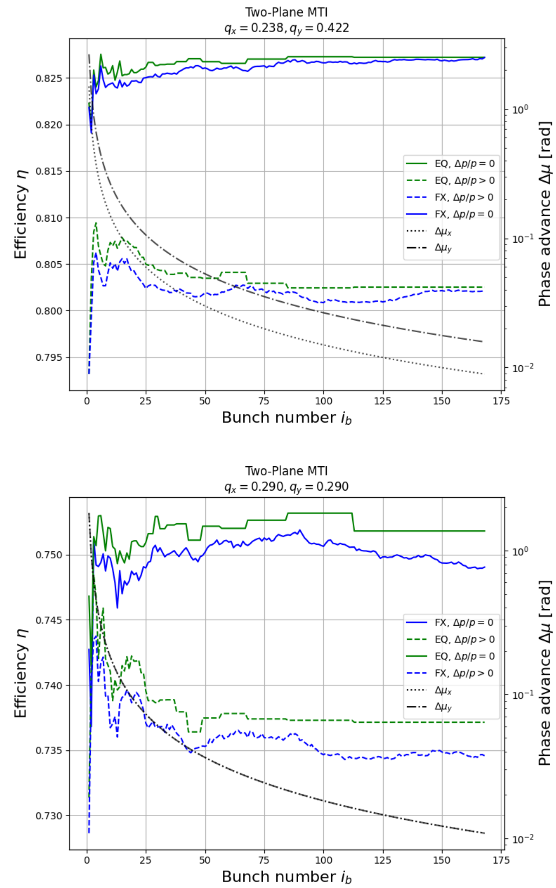

Figure 3: Same as Fig. 2, but for two-plane MTI.

OUTLOOK

An important extension of this work will be the inclusion of transverse and longitudinal space charge (SC) effects as well as a tune scan to find an optimal working point. An extension like this will show the relative influence of SC on the proposed injection models and which of the models will be superior. A full tune scan will show at which working point and which number of bunches the maximum efficiency will be reached.

ACKNOWLEDGEMENTS

One of the authors, AL, thanks Oleksiy Dolinskyy and Youssef El-Hayek for the very useful and constructive discussions on MTI and the practical support at GSI. The authors also thank the members of the accelerator physics group at the Institute of Applied Physics at the Goethe University Frankfurt for valuable discussions.

REFERENCES

[1] S. Appel and O. Boine-Frankenheim, "Optimization of multi-turn injection into a heavy-ion synchrotron using genetic algorithms", in *Proc. IPAC'15*, Richmond, VA, USA, May 2015, pp. 3689–3692. doi:10.18429/JACoW-IPAC2015-THPF007

[2] S. Appel, L. Groening, Y. E. Hayek, M. Maier, and C. Xiao, "Injection optimization through generation of flat ion beams", *Nucl. Instrum. Methods Phys. Res. A*, vol. 866, pp. 36–39, 2017. doi:10.1016/j.nima.2017.05.041

[3] Y. E. Hayek, "Minimierung der systemischen Anfangsverluste im SIS18", Ph.D. thesis, Goethe University Frankfurt, 2013.

[4] O. Dolinskyy, Y. E. Hayek, D. Ondreka, and P. Spiller, "Enhancing beam intensity in SIS18 by a two-plane multi-turn injection approach", in *Proc. IPAC'25*, Taipei, Taiwan, pp. 836–839, Nov. 2025. doi:10.18429/JACoW-IPAC2025-MOPS141

[5] S. Zhang *et al.*, "Simulation and parameter optimization of 6-dimensional phase space injection scheme based on HIAF-BRing", *Nucl. Instrum. Methods Phys. Res. A*, vol. 1064, 2024. doi:10.1016/j.nima.2024.169348

[6] GSI Helmholtzzentrum für Schwerionenforschung, "JUAS Lecture Notes: UNILAC", https://www-bd.gsi.de/conf/juas/juas_script.pdf